

UCSF

UC San Francisco Previously Published Works

Title

Molecular and Genetic Analyses of Collagen Type IV Mutant Mouse Models of Spontaneous Intracerebral Hemorrhage Identify Mechanisms for Stroke Prevention

Permalink

<https://escholarship.org/uc/item/4bk9t8jp>

Journal

Circulation, 131(18)

ISSN

0009-7322

Authors

Jeanne, Marion
Jorgensen, Jeff
Gould, Douglas B

Publication Date

2015-05-05

DOI

10.1161/circulationaha.114.013395

Peer reviewed

Molecular and Genetic Analyses of Collagen Type IV Mutant Mouse Models of Spontaneous Intracerebral Hemorrhage Identify Mechanisms for Stroke Prevention

Marion Jeanne, PhD; Jeff Jorgensen, BSc; Douglas B. Gould, PhD

Background—Collagen type IV alpha1 (COL4A1) and alpha2 (COL4A2) form heterotrimers critical for vascular basement membrane stability and function. Patients with *COL4A1* or *COL4A2* mutations suffer from diverse cerebrovascular diseases, including cerebral microbleeds, porencephaly, and fatal intracerebral hemorrhage (ICH). However, the pathogenic mechanisms remain unknown, and there is a lack of effective treatment.

Methods and Results—Using *Col4a1* and *Col4a2* mutant mouse models, we investigated the genetic complexity and cellular mechanisms underlying the disease. We found that *Col4a1* mutations cause abnormal vascular development, which triggers small-vessel disease, recurrent hemorrhagic strokes, and age-related macroangiopathy. We showed that allelic heterogeneity, genetic context, and environmental factors such as intense exercise or anticoagulant medication modulated disease severity and contributed to phenotypic heterogeneity. We found that intracellular accumulation of mutant collagen in vascular endothelial cells and pericytes was a key triggering factor of ICH. Finally, we showed that treatment of mutant mice with a US Food and Drug Administration–approved chemical chaperone resulted in a decreased collagen intracellular accumulation and a significant reduction in ICH severity.

Conclusions—Our data are the first to show therapeutic prevention in vivo of ICH resulting from *Col4a1* mutation and imply that a mechanism-based therapy promoting protein folding might also prevent ICH in patients with *COL4A1* and *COL4A2* mutations. (*Circulation*. 2015;131:1555-1565. DOI: 10.1161/CIRCULATIONAHA.114.013395.)

Key Words: cerebrovascular disorders ■ collagen ■ genetics ■ hemorrhage ■ stroke

Strokes cause a death every 4 minutes in the United States, representing the fourth leading cause of death and a major cause of long-term disability.¹ Intracerebral hemorrhages (ICHs) are the most fatal form of stroke.² Lack of effective treatment options and poor clinical outcomes for ICH patients suggest that prevention is paramount for reducing the tremendous personal and societal burden. Development of preventive strategies relies on understanding environmental and genetic factors that contribute to ICH risk. Mutations in the genes encoding collagen type IV alpha1 (COL4A1) and alpha2 (COL4A2) cause highly penetrant cerebrovascular disease with variable expressivity.³ *COL4A1* mutations are a significant cause of porencephaly⁴ and pediatric ICH, which are associated with particularly poor outcomes, including cerebral palsy, intellectual disabilities, developmental and behavioral disorders, and epilepsy. *COL4A1* and *COL4A2* mutations also cause spontaneous ICHs in adults.^{5,6} Thus, *COL4A1* and *COL4A2* mutations are important causes of highly penetrant perinatal ICH and may play a substantial role in age-related cerebrovascular diseases.

COL4A1 and COL4A2 are extracellular matrix molecules that form a network integral to basement membranes.^{7,8} They are cotranslationally translocated into the endoplasmic reticulum, where they assemble into heterotrimers composed of 1 COL4A2 and 2 COL4A1 molecules.⁹ Each protein has a large triple-helical domain flanked by the 7S¹⁰ and noncollagenous (NC1) domains at the amino and carboxy terminus, respectively.¹¹ The globular NC1 domains are responsible for initiating heterotrimer assembly, which proceeds by the progressive interwinding of the triple-helical domains.^{12,13} Triple-helical domains are characterized by repeated Gly-Xaa-Yaa motifs (Xaa and Yaa represent variable amino acids) and form >80% of the proteins. As in other collagens,^{14,15} glycine missense mutations are the most common type of mutation,¹⁶ and in vitro, the primary consequence appears to be impaired heterotrimer biosynthesis.^{5,17,18} How this may contribute to ICH in vivo remains unknown. Pathogenesis could involve toxic intracellular heterotrimer accumulation, extracellular deficiency of normal collagen, or the extracellular presence of mutant collagen.¹⁹ Our objectives were to identify the molecular and cellular events that occur in the neurovascular unit leading to ICH in *Col4a1* mutant mice and to identify

Clinical Perspective on p 1565

Received September 22, 2014; accepted February 26, 2015.

From Departments of Ophthalmology and Anatomy, Institute for Human Genetics, University of California, San Francisco (UCSF).

The online-only Data Supplement is available with this article at <http://circ.ahajournals.org/lookup/suppl/doi:10.1161/CIRCULATIONAHA.114.013395/-DC1>.

Correspondence to Douglas B. Gould, PhD, University of California, San Francisco, 10 Koret Way (K235), San Francisco, CA 94143-0730. E-mail GouldD@vision.ucsf.edu

© 2015 American Heart Association, Inc.

Circulation is available at <http://circ.ahajournals.org>

DOI: 10.1161/CIRCULATIONAHA.114.013395

preventive therapeutics that target these events. We investigated the timing and location of the pathogenesis and potential roles of intracellular and extracellular insults using multiple mouse models. Importantly, we identified modifiable ICH risk factors and a pharmacological intervention that reduced ICH in vivo. These data provide proof of principle for mechanism-based interventions to reduce, delay, or prevent ICH in patients with *COL4A1* and *COL4A2* mutations.

Methods

Animals

Procedures were in accordance with Institutional Animal Care and Use Committee guidelines. *Col4a1* and *Col4a2* mutant mice were described previously.^{18,20} Each strain was iteratively crossed to C57BL/6J (B6) mice for at least 5 generations. CAST/EiJ (CAST) and 129S6/SvEvTac (129) breeders were mated with B6 mice to produce CASTB6F1 and 129B6F1 mice, respectively. The *Col4a1*^{Flox41} conditional mutant mouse was produced by InGenious Targeting Laboratory (Stony Brook, NY). Rosa26-Cre^{ER} mice²¹ were used for ubiquitous inducible CRE expression. *Tie2-Cre*,²² *Pdgfrb-Cre*,²³ and *Gfap-Cre*²⁴ were used for cell-type specific CRE expression. We used ROSA26tm14(CAG-tdTomato) reporter mice²⁵ to validate CRE-mediated recombination. Unless specified, all mutant mice were heterozygous, and both sexes were used.

In Vivo Procedures

CRE was activated with tamoxifen (10 mg/mL; Sigma-Aldrich, St. Louis, MO). Pregnant females received 1 intraperitoneal tamoxifen injection (2 mg) mixed with progesterone (1 mg; Sigma-Aldrich). Pups received 1 intragastric tamoxifen injection (50 µg) for 3 consecutive days, and 3-week-old mice received 1 intraperitoneal tamoxifen injection (2 mg) for 2 consecutive days.

Virgin 3-month-old females were exercised on a horizontal treadmill (Exer 3/6, Columbus Instruments, Columbus, OH) for 5 sessions. Each session included a 2-minute acclimation period (speed, 0 m/min), 8-minute warmup (3 minutes at 6 m/min, 3 minutes at 9 m/min, 2 minutes at 12 m/min), and five 1-minute sprints (1 minute at 15 m/min followed by 1 minute rest at 0 m/min). Sessions were performed 5 days apart, and animals were euthanized 12 days after the last session.

Mice received Warfarin (warfarin sodium tablets, Amneal Pharmaceuticals, Bridgewater, NJ) via drinking water at the estimated dose of 0.4 mg/kg per day (2.5 mg dissolved in 800 mL water) for 4 days, water without warfarin for 2 days, and then water with warfarin for 3 days. Because 2 mutant mice died, treatment was discontinued, and the remaining animals were euthanized 11 days later.

Mice received sodium 4-phenylbutyrate (4PBA; Enzo Life Sciences Inc, Farmingdale, NY) diluted in PBS by injection. Pups received intragastric injection of 0.1 mg 4PBA at postnatal day (P) 1, P3, P5, and P7; then intraperitoneal injection of 0.5 mg 4PBA at P10, P12, P14, P16, P18, and P20; and finally intraperitoneal injection of 1.0 mg 4PBA at P23 and P26. Mice were euthanized at 1 month of age.

Retinal fluorescein angiography was performed with a Micron III (Phoenix Research Labs Inc, Pleasanton, CA). One-month-old mice were anesthetized with ketamine (100 mg/kg)-xylazine (10 mg/kg) and received an intraperitoneal 20-µL fluorescein sodium injection (25 mg/mL in PBS; Altaire Pharmaceuticals Inc, Riverhead, NY).

Histology and Immunofluorescence Labeling

Anesthetized mice were transcardially perfused with saline followed by 4% paraformaldehyde in PBS. Brains were postfixed in 4% paraformaldehyde for 16 hours, cryoprotected in 30% sucrose/PBS, and embedded in optimal cutting temperature (Sakura Finetek, Torrance, CA). For ICH quantification, coronal cryosections (35 µm) regularly spaced along the rostro-codal axis were stained with Prussian Blue/Fast red. Images were acquired with a Stereo Discovery.V8 microscope, an AxioCam ICc3 camera, and AxioVision 4.6 software (Carl

Zeiss Microscopy, LLC, Germany). On each section, the percentage of brain area with Prussian Blue staining was calculated with ImageJ software (National Institutes of Health). Hemorrhage severity was expressed as the average percentage of hemosiderin surface area on 27 sections for each brain. Trichrome staining was performed on 5-µm paraffin sections according to the manufacturer's protocol (One Step Trichrome Blue/Red Stain Kit, American Mastertech Scientific Inc, Lodi, CA).

For the investigation of blood-brain barrier integrity, 10 mL biotin (EZ-link sulfo-NHS-Biotin, 0.5 mg/mL in PBS; Thermo Scientific, Waltham, MA) was transcardially perfused after washing with saline and before fixation with 4% paraformaldehyde. Coronal cryosections were fixed 15 minutes in 4% paraformaldehyde and labeled with streptavidin Alexa Fluor 488 (2 µg/µL; Invitrogen-Molecular Probes, Carlsbad, CA). Alternatively, a 2% Evans Blue solution in saline (4 mL/kg) was injected intraperitoneally and allowed to circulate for 24 hours.

Embryos were fixed for 1 hour in cold methanol, cryoprotected in 30% sucrose/PBS, and cryosectioned (20 µm). For embryonic angiogenesis, hindbrains were fixed for 1 hour in 4% paraformaldehyde before flat mounting. For retinal analysis, enucleated eyes were fixed for 16 hours in 4% paraformaldehyde, and dissected retinas were flat mounted. Cultured primary fibroblasts were fixed for 15 minutes in 4% paraformaldehyde and permeabilized in PBS/0.1% Triton X-100 before immunolabeling. Cryosections were postfixed in 4% paraformaldehyde for 15 minutes before immunolabeling. All specimens were blocked in PBS with 10% normal donkey serum, 1% BSA, and 0.3% Triton X-100. Primary antibodies—rat CD31 (1:200; BD Biosciences, San Jose, CA), goat type IV collagen (1:200; Southern Biotech, Birmingham, AL), rat COL4A1 (1:100, H11 clone; Shigei Medical Research Institute, Okayama, Japan²⁶), rabbit ZO-1 (1:100; Abcam, Cambridge, UK), rabbit Claudin5 (1:100; Invitrogen, Carlsbad, CA), and mouse HSP47 (1:500, M16.10A1 clone; Stressgen Biotechnologies, San Diego, CA)—were incubated for 3 hours at room temperature for cryosections or for 48 hours at 4°C for flat mounts. After 3 washes in PBS/0.1% Triton X-100, secondary antibodies—Alexa Fluor 488 or 594 (1:500 dilution; Invitrogen-Molecular Probes)—were incubated for 1 hour for sections or 24 hours for flat mounts. After 3 washes, coverslips were mounted with Mowiol with DAPI (2 µg/mL). A Zeiss AxioImager M.1 and a Zeiss LSM700 with plan-Apochromat objectives (63×/1.4 oil immersion or 20×/0.8) were used for fluorescence microscopy, with an AxioCam MRm camera and AxioVision and ZEN software (Carl Zeiss Microscopy, LLC). Embryonic vascular plexus density quantifications were performed with ImageJ. Vein branch point quantifications were realized by averaging the number of at least 3 primary veins per retina.

Western Blot Analysis

Mouse embryonic fibroblasts were cultured in Dulbecco modified Eagle medium with 10% FBS, 2 mmol/L L-glutamine, and 0.2 mmol/L penicillin/streptomycin at 37°C in 5% CO₂. At confluence, cells were serum deprived and treated with 50 µg/mL ascorbic acid for 16 hours. Proteins were separated on 4% to 15% gradient SDS-PAGE gels (Bio-Rad Laboratories Inc, Hercules, CA). Membranes were blocked for 16 hours in Tris-buffered saline/0.1% Tween-20 with 5% nonfat milk and then incubated for 16 hours with the following primary antibodies: rat COL4A1 (1:200, H11 clone; Shigei Medical Research Institute²⁶), tubulin (1:10000, T6557; Sigma-Aldrich), and laminin (1+2; 1:2000, ab7463; Abcam). After 3 washes in Tris-buffered saline/0.1% Tween-20, membranes were incubated for 1 hour with horseradish peroxidase-conjugated secondary antibodies (1:10000; Jackson ImmunoResearch, West Grove, PA). After 3 washes, SuperSignal West Pico Chemiluminescent substrate (Thermo Scientific) was used according to the manufacturer's instructions.

Statistical Analysis

Normality was assessed with the Kolmogorov-Smirnov and Shapiro-Wilk tests. Two-group comparisons were carried out with the Student *t* test. Multiple-group comparisons were performed with ANOVA followed by the Tukey posttest or Kruskal-Wallis

test followed by the Dunn posttest for normally and not normally distributed variables, respectively. Values of $P < 0.05$ were considered statistically significant. Data are presented as mean+SD or mean±SD.

Results

Pathogenesis Occurs in Distinct Stages

Col4a1^{Δex41} is a splice-site mutation that skips exon 41 in the triple-helical domain of murine *Col4a1*.^{3,17,27} *Col4a1*^{Δex41/Δex41} mice die during embryogenesis, and *Col4a1*^{+Δex41} mice exhibit embryonic growth retardation and reduced postnatal viability (Figure I in the online-only Data Supplement). Modeling patients with *COL4A1* mutations, surviving *Col4a1*^{+Δex41} mice have multisystem disorders, including fully penetrant cerebrovascular disease presenting as porencephaly and prenatal, perinatal, and recurrent multifocal ICHs.^{17,27} At embryonic day (E) 10.5, we observed irregularly shaped and enlarged blood vessels, as well as multifocal intraparenchymal and intraventricular hemorrhages (Figure 1A). Analysis of cerebral angiogenesis at E12.5 revealed increased vessel density and tortuosity in *Col4a1*^{+Δex41} hindbrains (Figure 1B). Mature retinal vasculature showed similar defects, including persistent hyaloid vessels and abnormal crossing of excessively branched, tortuous arteries, and veins with irregular diameters (Figure 1C). We also detected tortuous cerebral

arteries, veins, and capillaries in adult *Col4a1*^{+Δex41} mice (Figure 1D). Cerebral and retinal vessels were not permeable to biotin, Evans Blue dye, or sodium fluorescein, and tight junction proteins were normally expressed during brain development, indicating that the blood-brain and blood-retinal barriers are intact (Figure 1D and Figure II in the online-only Data Supplement).

At birth, *Col4a1*^{+Δex41} pups had numerous macroscopic subcutaneous hematomas, extra-axial hemorrhages, and frequent intraparenchymal hemorrhages (Figure 1C in the online-only Data Supplement). Consistent with highly penetrant intraventricular hemorrhages, 80% of *Col4a1*^{+Δex41} mice had porencephaly (Figure 2A). ICH was completely penetrant; however, the location and character of the lesions changed with time, suggesting different stages of pathology. At 1 month, *Col4a1*^{+Δex41} mice had small-vessel disease, with multiple small hemosiderin deposits throughout the cortex, cerebral nuclei, brainstem, and cerebellum. By 3 months, these were cleared, but fewer and larger hemorrhages appeared in the basal ganglia. Reduced hemoglobin level and age-dependent hemosiderin accumulation indicated recurring ICHs (Figure 2A and Figure III in the online-only Data Supplement). Importantly, cerebral macroangiopathy with fibrotic vessel wall thickening and thrombus formation appeared with age (Figure 2B).

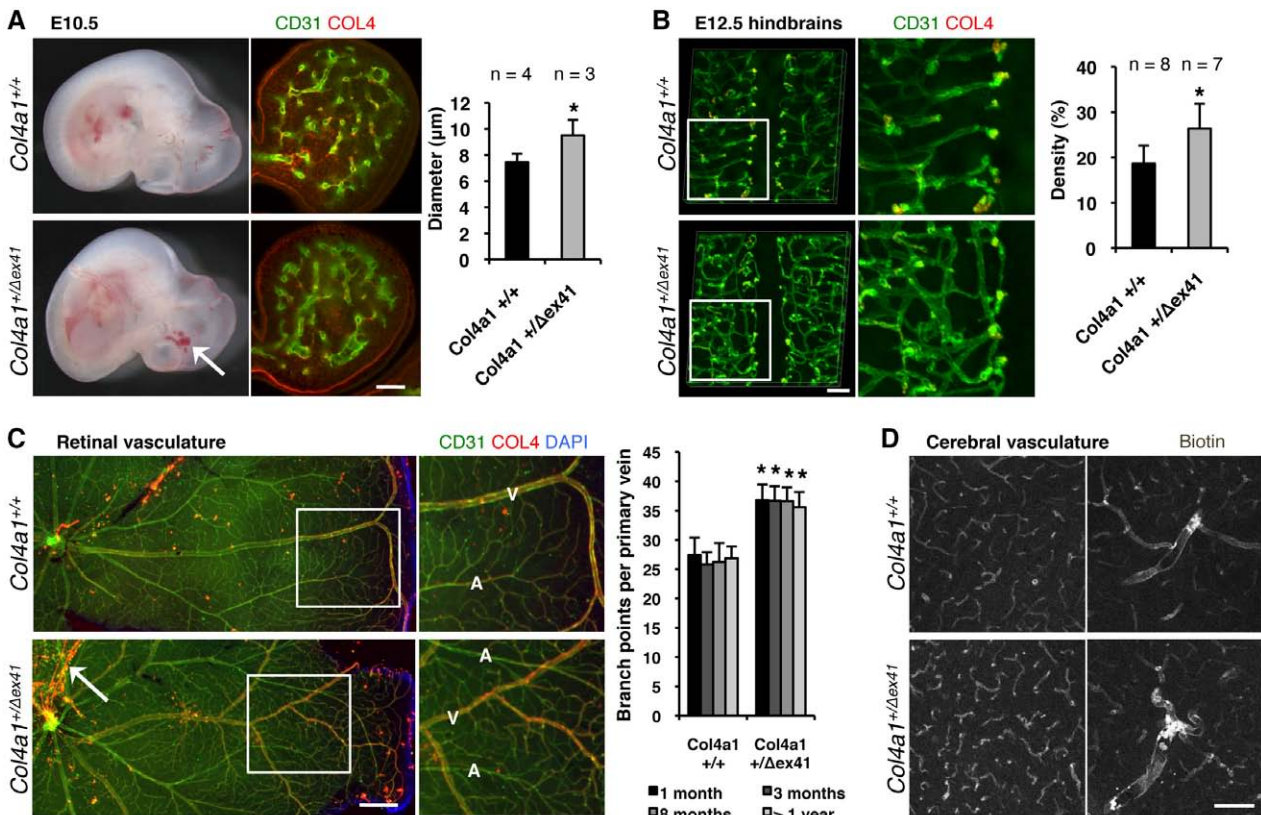


Figure 1. *Col4a1* mutation causes abnormal cerebral and retinal vascular development. **A**, At embryonic day (E) 10.5, *Col4a1*^{+Δex41} mice have irregularly shaped, enlarged blood vessels (calculated in branchial arches using CD31 and collagen type IV [COL4] labeling; scale bar, 100 μm) and intracerebral hemorrhages (arrow). **B**, At E12.5, *Col4a1*^{+Δex41} mice have abnormally tortuous vessels with increased density (calculated in hindbrain flat mounts with CD31 labeling; scale bar, 100 μm). **C**, In mutant animals, retinal blood vessels are tortuous, arteries (A) and veins (V) cross each other, and there is excess branching in the main veins (5≤n≤16, pair-wise comparisons per age; scale bar, 500 μm). **D**, Intracardiac perfusion of biotin revealed that adult mutant animals have tortuous cerebral blood vessels without a compromised blood-brain barrier (scale bar, 100 μm). Data are reported as mean+SD. * $P < 0.05$ vs *Col4a1*^{+/+} by the Student *t* test.

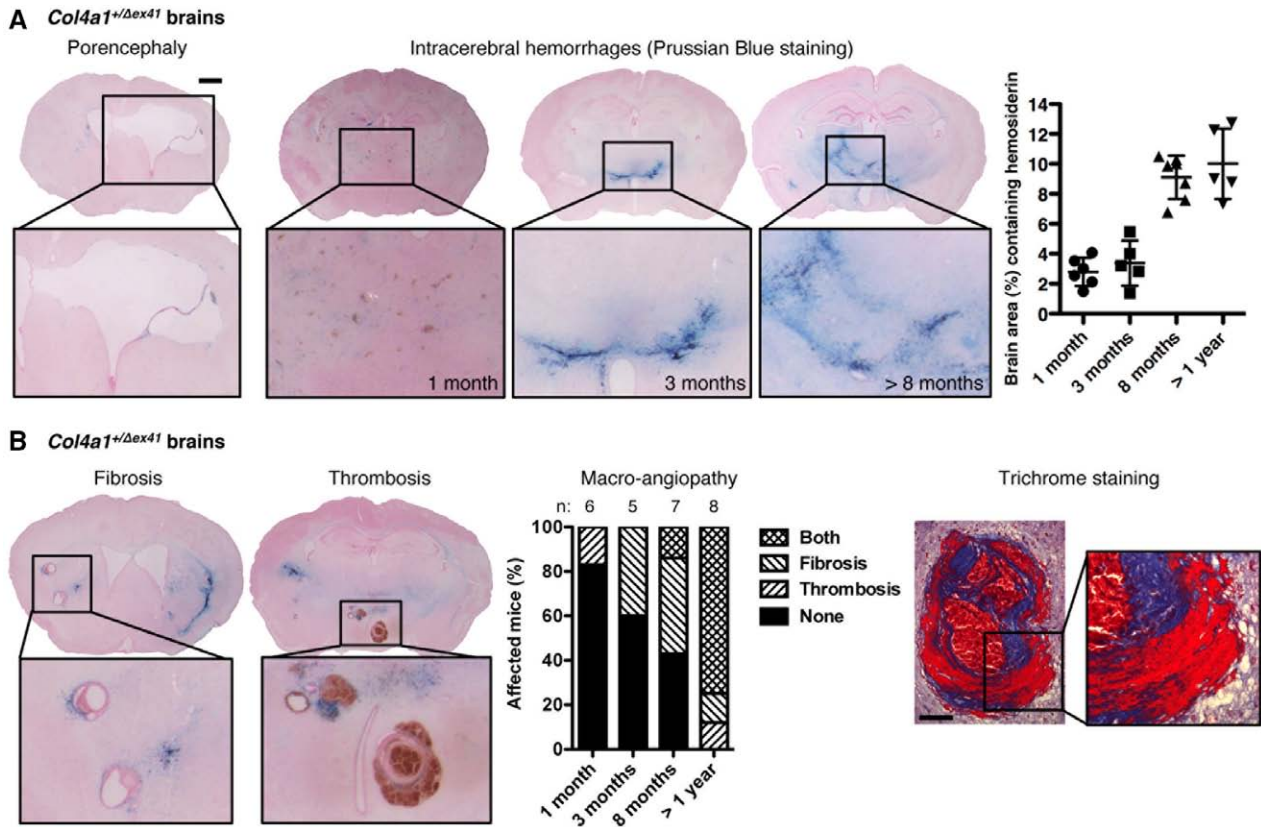


Figure 2. *Col4a1* mutation causes small-vessel disease, hemorrhagic stroke, and macroangiopathy. **A**, *Col4a1*^{+/ Δ ex41} mice have porencephaly (penetrance, 80%) and intracerebral hemorrhages (penetrance, 100%) quantified with Prussian Blue staining of serial coronal brain sections (scale bar, 1 mm). Data are reported as mean \pm SD. **B**, Macroangiopathy with vessel wall thickening, fibrosis, and thrombosis advanced with age. Trichrome staining shows collagen deposition (blue) and fibrin accumulation (red) in affected blood vessels (scale bar, 100 μ m). No *Col4a1*^{+/+} mice had porencephaly, intracerebral hemorrhage, or macroangiopathy (n=32).

Age-Related ICH and Macroangiopathy Are Consequences of Developmental Defects

To distinguish between potentially distinct roles for COL4A1 in cerebrovascular development and maintenance, we engineered a conditional *Col4a1* mutation by flanking exon 41 with *LoxP* sites (*Col4a1*^{Flex41}). This allele recreates the *Col4a1* ^{Δ ex41} mutation in a CRE-dependent manner (Figure IV in the online-only Data Supplement). We crossed *Col4a1*^{Flex41} mice to the inducible, ubiquitous CRE strain *R26-Cre*^{ER} 21; injected tamoxifen at birth, 1 week, or 3 weeks; validated CRE activation; and quantified retinal branching and ICHs (Figure 3 and Figure V in the online-only Data Supplement). In 8-month-old *R26-Cre*^{ER}; *Col4a1*^{Flex41} mice, ICHs were more severe in mice that started to express mutant collagen at birth than at 1 week and were absent in mice that started to express mutant collagen at 3 weeks. Pathology in neither group was as severe as in *Col4a1*^{+/ Δ ex41}, and none of the mice had porencephaly or macroangiopathy. These data demonstrate that age-related, recurrent ICHs and macroangiopathy do not occur in the absence of prenatal and postnatal developmental defects. To refine the timing of pathogenesis, we induced the *Col4a1* mutation at E10.5 or E14.5 and quantified ICHs at 1 month. ICHs were more severe in mice induced at E10.5 than at E14.5. Again, neither group was as severe as *Col4a1*^{+/ Δ ex41}; however, controls revealed reduced recombination efficiency with embryonic induction of mutant *Col4a1* (Figure V in the online-only Data

Supplement). Together, these data demonstrate that the effects of mutant COL4A1 require expression during embryogenesis and the early postnatal period to cause progressive, recurrent ICHs and age-related macroangiopathy.

ICH Modulation by Environmental and Genetic Factors

We sought ways to reduce the severity of progressive ICH. In the previous experiment, tamoxifen injection during pregnancy compromised natural birth and necessitated surgical delivery. A beneficial effect of surgical delivery was previously proposed but not quantified.²⁷ We found that tamoxifen-treated, surgically delivered *Col4a1*^{+/ Δ ex41} mice had less ICHs than nontreated, naturally born *Col4a1*^{+/ Δ ex41} mice (Figure 4A). Next, we quantified the impacts of other modifiable risk factors that have been anecdotally associated with ICH in patients with *COL4A1* or *COL4A2* mutations, including physical exertion^{28–30} and anticoagulant administration.^{5,6,27,31} We found that exercise increased ICH severity (Figure 4B) and anticoagulants provoked fatal hemorrhages within just 7 days of use (Figure 4C). Together, these data establish vaginal delivery, exercise, and anticoagulants as modifiable risk factors that increase ICH severity in *Col4a1*^{+/ Δ ex41} mice.

Genetic factors may also influence clinical heterogeneity among patients with *COL4A1* and *COL4A2* mutations^{32,33} and can reveal pathogenic mechanisms and interventional

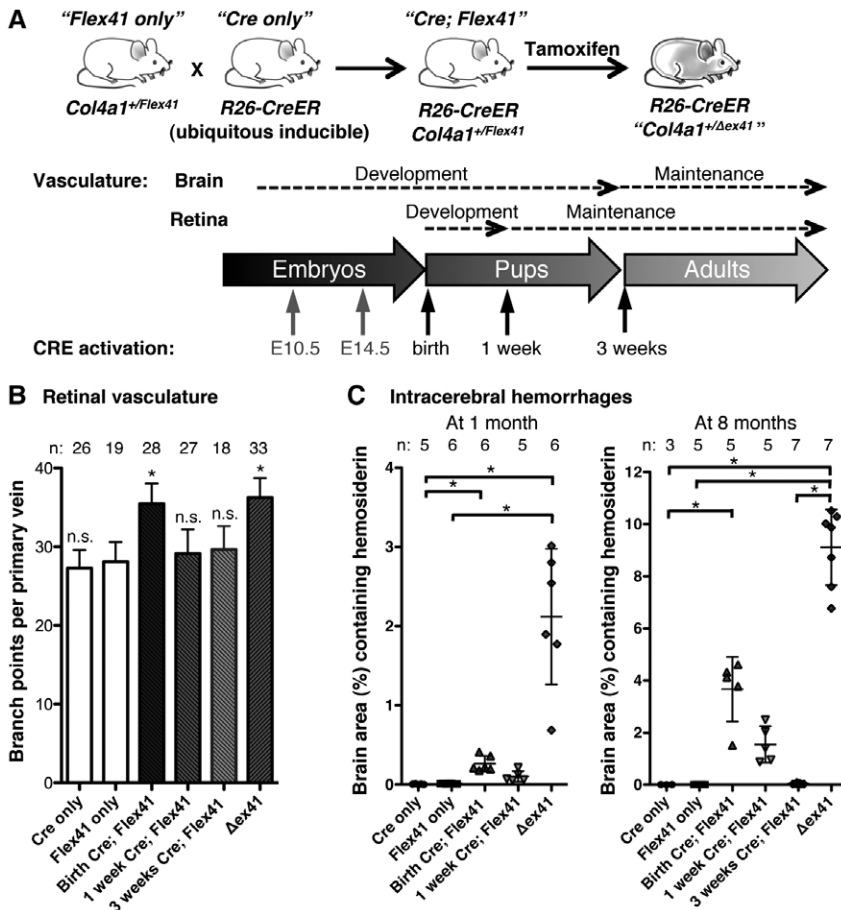


Figure 3. Mutant *Col4a1* causes cerebrovascular disease when expressed during vascular development. **A**, *Col4a1^{+/Flex41}* conditional mutant mice were crossed to *R26-CreER* ubiquitous inducible CRE mice, and the CRE recombinase was activated at different time points during or after vascular development by tamoxifen injections. **B**, Quantification of retinal vessels revealed excess branching in mice that started to express mutant COL4A1 at birth but not at 1 or 3 weeks. n.s. indicates $P > 0.05$; * $P < 0.05$ vs Flex41 only (*Col4a1^{+/Flex41}; R26-CreER^{-/-}*) mice by the Student *t* test. **C**, Intracerebral hemorrhage (ICH) quantification at 1 or 8 months of age shows that ICH severity increases with earlier age of expression of the collagen mutation. * $P < 0.05$ by Kruskal-Wallis test followed by Dunn posttest. Data are reported as mean ± SD.

approaches. We compared ICH severity in mice with different mutations on the same genetic background and in mice with the same mutation on different genetic backgrounds. The allelic series comprised *Col4a1^{Δex41}*, 7 glycine mutations in the triple-helical domain (6 in COL4A1, 1 in COL4A2) and 1 mutation in the COL4A1 NC1 domain (Figure 5A).^{18,20} We backcrossed each strain to C57BL/6J (B6) mice, aged the cohorts for 7.5 to 9.5 months (called the 8-month cohort), and compared pencephaly, ICH, and macroangiopathy. We identified distinct classes of mutations and 3 potential genotype-phenotype correlations (Figure 5A and Figure VI in the online-only Data

Supplement). First, there appears to be a class effect whereby *Col4a1^{Δex41}* is more severe than missense mutations. Second is a domain effect whereby the NC1 domain mutation is milder than the triple-helical domain mutations. Third, for mutations within the triple-helical domain, there was a position effect whereby mutations closer to the carboxy terminus were more severe than mutations closer to the amino terminus. These data establish the powerful effects of allelic heterogeneity on ICH severity and suggest that there are class, domain, and position effects of different alleles that resemble effects observed in other types of collagens.^{19,34–36} Next, we tested the effect of

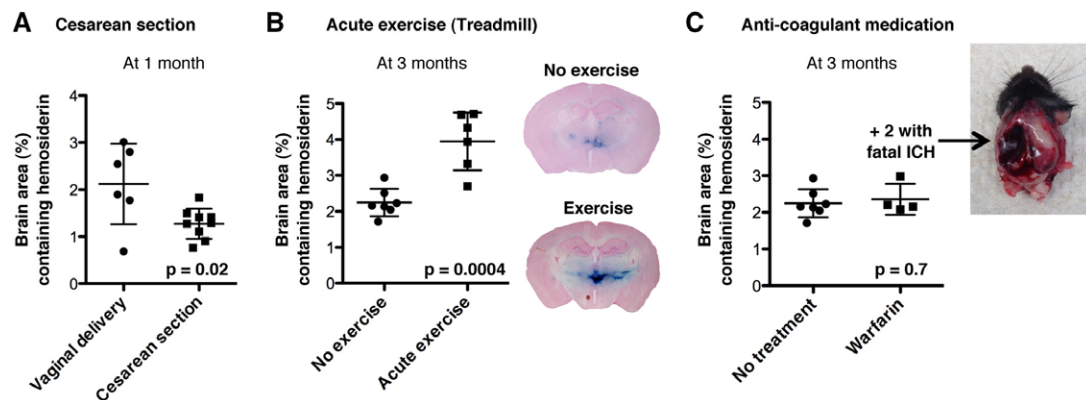


Figure 4. Environmental factors contribute to *Col4a1* mutation expressivity. Intracerebral hemorrhage quantification in *Col4a1^{+/Δex41}* mice: (A) after vaginal delivery or cesarean section, (B) without or with 5 sessions of five 1-minute sprints on a treadmill, and (C) without or with 7 days of warfarin anticoagulant administration. Data are reported as mean ± SD.

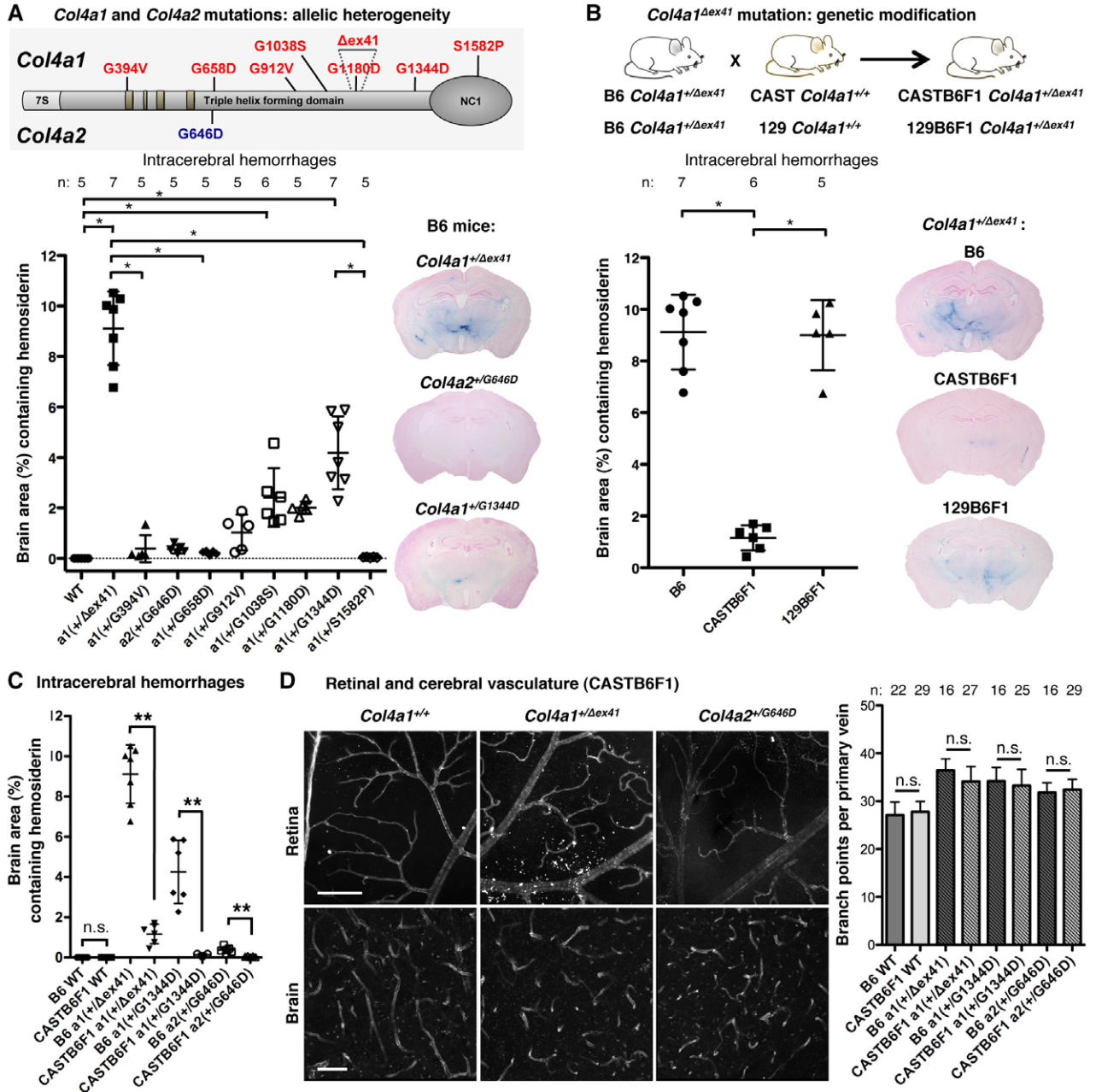


Figure 5. Allelic heterogeneity and genetic context contribute to the expressivity of *Col4a1* and *Col4a2* mutations. **A**, Intracerebral hemorrhage (ICH) quantification in 8-month-old mice with different mutations but the same genetic background, C57BL/6J (B6), demonstrates that allelic heterogeneity influences ICH severity. * $P < 0.05$ by Kruskal-Wallis test followed by Dunn posttest. **B**, ICH quantification in 8-month-old mice with the same *Col4a1*^{Δex41} mutation but different genetic contexts shows that genetic background influences ICH severity. A cross for 1 generation to CAST/EiJ (CAST) but not 129S6/SvEvTac (129) mice was sufficient to reduce ICH severity compared with *Col4a1*^{+/Δex41} mice on a B6 background. * $P < 0.05$ by ANOVA followed by Tukey posttest. **C**, CAST suppression of ICH was consistent across different mutations but **(D)** did not extend to prevention of vascular tortuosity and excess branching (collagen type IV [COL4] labeling in the retina, CD31 labeling in the brain; scale bars, 50 μ m). In **C** and **D**, n.s. indicates $P > 0.05$; ** $P < 0.01$ by the Student *t* test. Data are reported as mean \pm SD (**A–C**) or mean \pm SD (**D**). WT indicates wild-type.

genetic context on ICH severity. We crossed B6 *Col4a1*^{+/Δex41} mice to CAST/EiJ (CAST) or 129S6/SvEvTac (129) mice to generate CASTB6F1 or 129B6F1 mice, respectively. We compared ICH severity among *Col4a1*^{+/Δex41} mice and found that CASTB6F1 genetic context significantly suppressed ICH but 129B6F1 did not (Figure 5B). CASTB6F1 also reduced porencephaly penetrance and delayed macroangiopathy onset (Figure VII in the online-only Data Supplement). The effect

was not allele or gene specific because CASTB6F1 also significantly suppressed ICH in *Col4a1*^{+/G1344D} and *Col4a2*^{+/G646D} mice (Figure 5C). Surprisingly, there were neither allelic nor genetic context effects on retinal or cerebral blood vessel defects (Figure 5D). The observations of allelic and genetic context effects on ICH but not on the vascular patterning defects suggest that processes in addition to defective angiogenesis and vascular patterning may be required for ICH progression.

Pathogenic Collagen Accumulation in Vascular Endothelial Cells and Pericytes

Heterotrimers that incorporate mutant COL4A1 or COL4A2 tend to accumulate within cells at the expense of secretion. Because ICH severity correlates with intracellular accumulation in the allelic series,¹⁸ we hypothesized that CASTB6F1 suppression of ICH might occur by reducing intracellular COL4A1. We compared intracellular and extracellular COL4A1 in primary fibroblasts and found that *Col4a1*^{+/ Δ ex41} caused significantly increased intracellular COL4A1 in B6 but not CASTB6F1 cells (Figure 6A). Moreover, the CASTB6F1 background normalized intracellular without increasing extracellular COL4A1 levels, a distinction that was also striking in vivo. Blood vessels from B6 *Col4a1*^{+/ Δ ex41} animals had punctuate intracellular COL4 labeling and less intense labeling of the vascular basement membrane than *Col4a1*^{+/+} mice.

CASTB6F1 *Col4a1*^{+/ Δ ex41} vessels do not show intracellular labeling yet still lacked intense labeling of the basement membrane (Figure 6B). Thus, mutant mice from both backgrounds have reduced extracellular COL4A1, yet only B6 mice have significant intracellular accumulation and severe ICH. Importantly, these data dissect the potential roles of intracellular accumulation and extracellular deficiency and suggest that chronic intracellular accumulation may cause ICH in the context of developmentally abnormal vessels.

To test the relative effects of the different cell types of the neurovascular unit, we conditionally expressed mutant *Col4a1* in vascular endothelial cells (VECs), pericytes, or astrocytes using *Tie2-Cre*,²² *Pdgfrb-Cre*,²³ or *Gfap-Cre*²⁴ transgenic mice, respectively (Figure 6C). We validated these lines (Figure VIIIA in the online-only Data Supplement) and quantified ICH at 1 and 8 months. Specific expression of mutant

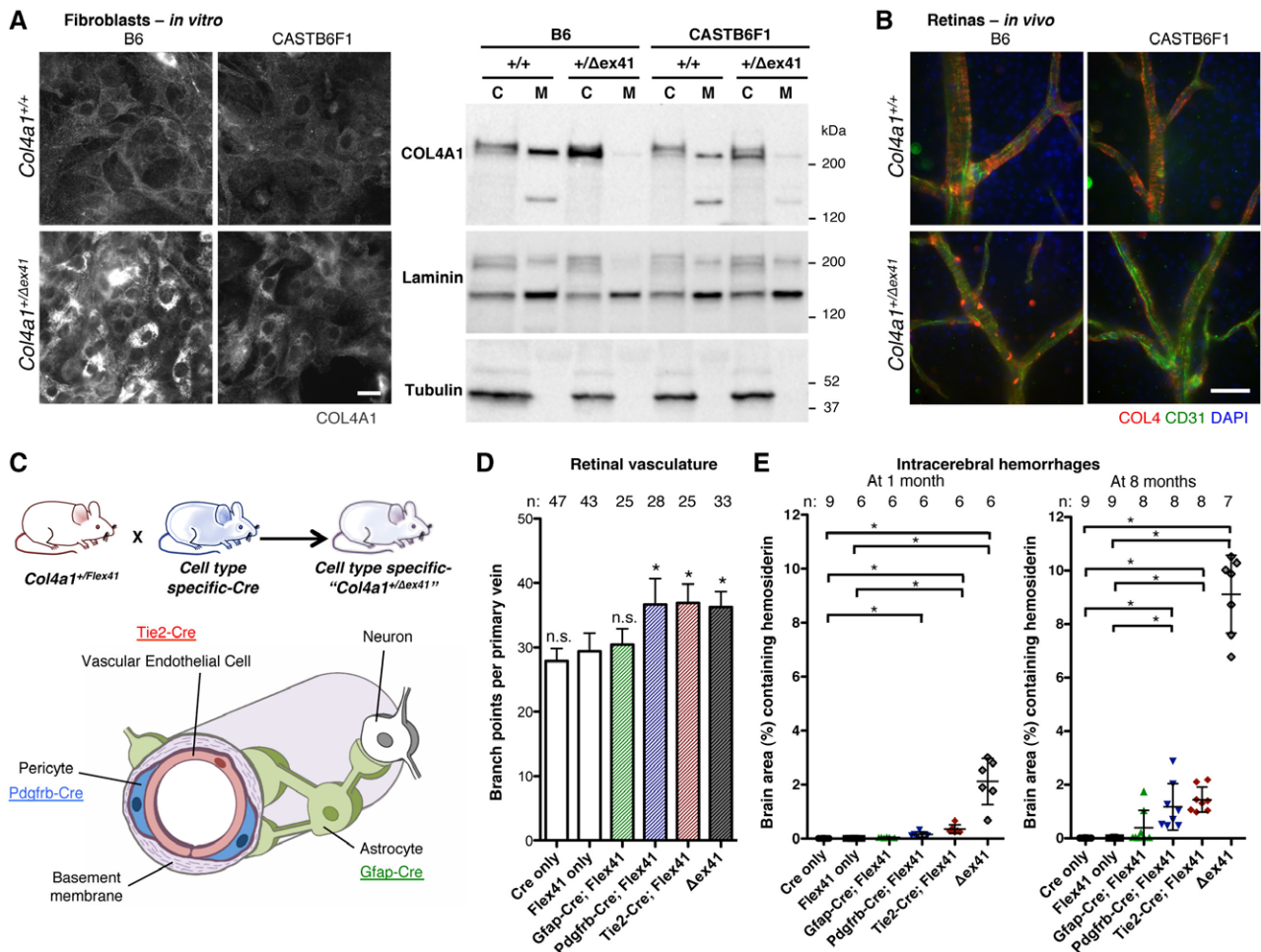


Figure 6. Intracerebral hemorrhages (ICHs) are associated with intracellular COL4A1 accumulation in vascular endothelial cells (VECs) and pericytes but not with extracellular deficiency. **A**, Immunolabeling and Western blot show that intracellular COL4A1 in *Col4a1*^{+/ Δ ex41} cells from B6 mice is greatly reduced in cells from CASTB6F1 mice but without an obvious increase in extracellular COL4A1. Laminin and tubulin are controls for secreted and intracellular proteins, respectively. Results constitute representative examples from 12 independent biological replicates obtained from 3 independent experiments. **C** indicates cell lysate; and M, conditioned medium. **B**, Immunolabeling of *Col4a1*^{+/ Δ ex41} retinal vessels shows strong intracellular collagen type IV (COL4) in B6 but not CASTB6F1 mice. **C**, *Col4a1*^{+/ Δ ex41} mice were crossed to *Tie2-Cre*, *Pdgfrb-Cre*, or *Gfap-Cre* strains for mutant *Col4a1* conditional expression in VECs, pericytes, or astrocytes, respectively. **D**, Retinal vessel quantification revealed excess branching with mutant expression in VECs and pericytes but not astrocytes. n.s. indicates $P > 0.05$; * $P < 0.05$ vs Flex41-only mice (*Col4a1*^{+/ Δ ex41}; Cre^{-/-}) by Student *t* test. **E**, ICH quantification demonstrated that mutant *Col4a1* expression in VECs or pericytes is sufficient to cause ICH but that neither cell type alone phenocopies *Col4a1*^{+/ Δ ex41}. Conditional expression of mutant *Col4a1* in astrocytes caused very mild ICHs in only three 8-month-old animals. * $P < 0.05$ by Kruskal-Wallis test followed by Dunn posttest. Scale bars, 50 μ m. Data are reported as mean+SD (**D**) or mean \pm SD (**E**).

Col4a1 only in astrocytes did not overall significantly affect retinal branching and gave very mild ICHs in only 3 of 8 old animals (Figure 6D and 6E). Expression in VECs-only or pericytes-only was sufficient to phenocopy excess retinal vascular branching of *Col4a1*^{+/ Δ ex41} (Figure 6D) and caused fully penetrant ICH (Figure 6E) and incompletely penetrant porencephaly and macroangiopathy (Figure VIII B in the online-only Data Supplement). However neither strain demonstrated ICH as severe as that in *Col4a1*^{+/ Δ ex41} mice. Interestingly, when we tested E16.5 embryos, ICH was greater in *Tie2-Cre;Col4a1*^{+/ Δ ex41} compared to *Pdgfrb-Cre;Col4a1*^{+/ Δ ex41} mice, and the postnatal viability of *Tie2-Cre;Col4a1*^{+/ Δ ex41} mice was much lower (27% compared with 100% for *Pdgfrb-Cre;Col4a1*^{+/ Δ ex41} mice; Figure IVD in the online-only Data Supplement). Therefore, the most severely affected *Tie2-Cre;Col4a1*^{+/ Δ ex41} mice may be underrepresented in postnatal analyses, leading to an underestimate of the relative role of VECs in the pathogenesis. These data suggest that both VECs and pericytes contribute to vascular defects and that VECs may play a relatively larger role.

The results from CASTB6F1 mice suggest that reducing intracellular accumulation may suppress ICH, and results from the inducible mutation indicate that postnatal intervention may be effective. 4PBA, a US Food and Drug Administration–approved chemical chaperone, has been used in several models of disorders caused by protein misfolding,³⁷ and we recently showed that its properties extend to COL4A1 in vitro.¹⁸ To test our hypothesis in vivo, we treated pups with 4PBA from birth to weaning age and analyzed retinal vasculature and ICH at 1 month. Treatment had no effect on vessel branching; however, there was decreased intracellular accumulation and qualitatively more uniform labeling of vascular basement membranes. Importantly, compared with untreated *Col4a1*^{+/ Δ ex41} mice, mutant animals treated with 4PBA had significantly less severe ICH (Figure 7). These data are the first to show therapeutic prevention of *Col4a1*-related ICH in vivo and support the hypothesis that promoting protein

folding might also prevent ICH in patients with *COL4A1* and *COL4A2* mutations.

Discussion

Col4a1 and *Col4a2* mutant mice model important aspects of human disease. Embryonic germinal matrix hemorrhages cause porencephaly, and early small-vessel disease presents as microbleeds throughout the brain. Later, recurrent ICHs and age-related macroangiopathy occur mainly in the basal ganglia. Importantly, our data bring new insights into the disease biology and suggest that 2 pathogenic mechanisms are necessary to cause ICH. First, we showed that *Col4a1* and *Col4a2* mutations cause abnormal angiogenesis. The fact that mice that start to express mutant collagen after the completion of vascular development do not suffer from ICH suggests that abnormal angiogenesis is required to trigger hemorrhage. Second, we showed that *Col4a1* mutation causes increased intracellular and decreased extracellular collagen. The fact that ICH severity is associated with the level of intracellular accumulation but not with extracellular deficiency (Figures 5B, 6A, and 6B) suggests that the intracellular accumulation is a key molecular mechanism in the progression to vasculature rupture. A similar observation was reported in human cells cultured from an ICH patient with a *COL4A2* mutation and his unaffected father who also carried the mutation.³⁸ The fact that the blood-brain barrier of the abnormally developed vessels is generally not compromised also supports this hypothesis, suggesting that chronic intracellular accumulation could reach locally toxic thresholds and provoke focal ICH. Interestingly, we show that abnormal angiogenesis is independent of the level of intracellular collagen accumulation, suggesting that extracellular insults might underlie abnormal vascular development. To support this hypothesis, it would be interesting to investigate the COL4A1/COL4A2 network in the vascular basement membrane. Indeed, this network has been shown to interact directly with several signaling pathways involved in angiogenesis such as transforming growth factor- β /brain

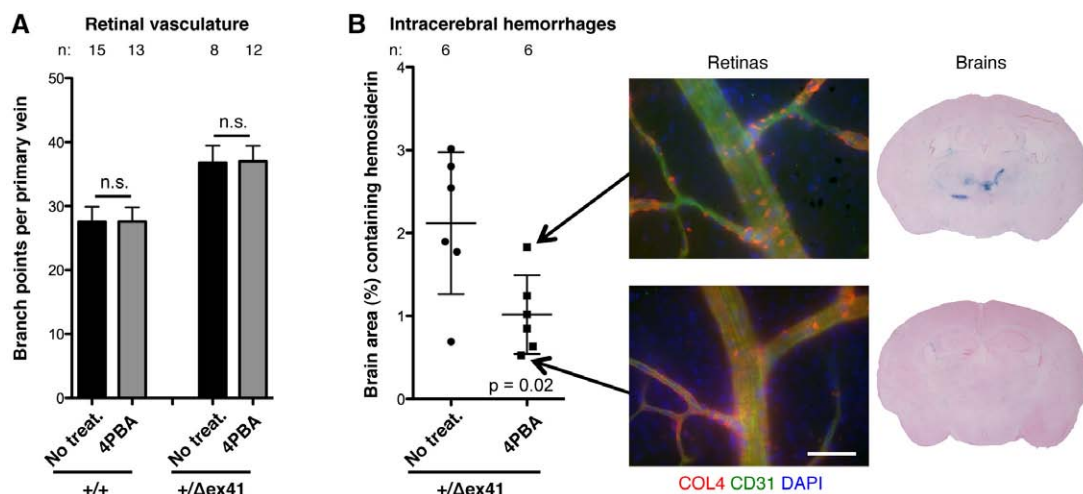


Figure 7. Treatment with chemical chaperone sodium 4-phenylbutyrate (4PBA) reduces intracerebral hemorrhage (ICH) severity in vivo. *Col4a1*^{+/ Δ ex41} mice treated from birth to 3 weeks with 4PBA had similar levels of retinal vessel branching (A) but less severe ICHs (B) compared with untreated *Col4a1*^{+/ Δ ex41} mice. Immunolabeled vessels showed less intracellular and more extracellular collagen type IV (COL4) in the treated *Col4a1*^{+/ Δ ex41} mouse with the least, compared with greatest, ICH severity. Scale bars, 50 μ m. Data are reported as mean \pm SD (A) or mean \pm SD (B). n.s. indicates $P>0.05$ by Student t test.

morphogenetic protein signaling,^{39,40} Notch signaling,⁴¹ and integrin signaling,⁴² and arresten, a proteolytic fragment of COL4A1, has antiangiogenic properties.⁴³ Although further understanding the roles of COL4A1 and COL4A2 in angiogenesis is compelling, developmental defects remain challenging to target therapeutically. Thus, we showed that targeting intracellular collagen accumulation with 4PBA, even after birth, successfully decreases ICH severity in vivo. These data support that mechanism-based treatments such as chemical chaperones might also prevent ICH in patients with COL4A1 and COL4A2 mutations.

We investigated a clinically relevant series of *Col4a1* and *Col4a2* mutations and discovered important allelic effects that resemble those identified for other type of collagens.^{19,34–36} These data have implications for patient screening and for functionally validating mutations that are identified by genetic testing. We show that mutation class, domain, and position all influence ICH severity and correlate with intracellular accumulation of heterotrimers.¹⁸ Mutations that are near the amino terminus of the triple-helical domain may cause only mild intracellular collagen accumulation and therefore may be overlooked by functional assays that measure relative levels of intracellular collagen, resulting in false negatives (eg, *Col4a1*^{+G394V}).¹⁸ Therefore, position effects should be considered when functionally testing putative mutations, and the incidence of COL4A1 and COL4A2 mutations may be higher than current estimates. Interestingly, despite differences in stoichiometric contributions to heterotrimer composition, positionally matched mutations in *Col4a1* and *Col4a2* caused similar ICH severity, which underscores the importance of analyzing both genes when genetically screening patients.

Importantly, our data suggest that the mechanism by which COL4A1 and COL4A2 mutations cause ICH might be specific to this phenotype, which may have important implications for patient prognosis and treatment. First, 129B6F1 genetic context modified ocular dysgenesis³² but not ICH. Second, in the allelic series, ICH severity correlates with levels of intracellular accumulation, whereas myopathy does not.¹⁸ This is illustrated by *Col4a1*^{G394V}, which is among the mutations causing the most severe myopathy but the least severe ICH. HANAC (hereditary angiopathy, nephropathy, aneurysms, and cramps) describes a subset of patients with myopathy and relatively mild cerebrovascular disease whose mutations cluster near integrin-binding domains in the amino-terminal quarter of COL4A1. Our data (Figure 5A and the work by Kuo et al¹⁸) suggest a molecular explanation for HANAC whereby mutations in or near integrin-binding domains lead to myopathy, and because these domains are near the amino terminus, the mutations cause only mild intracellular collagen accumulation and relatively mild ICH. Mechanistic heterogeneity has important implications for targeted therapies and patient treatment. These results suggest that pharmacological interventions that prevent ICH might not be efficacious for other phenotypes and that comprehensive patient treatment might require distinct approaches for distinct pathologies.

We have identified vaginal delivery, intense exercise, and anticoagulant use as modifiable environmental risk factors that exacerbate ICH severity in *Col4a1*^{+Δex41} mice. Anticoagulation is a highly effective treatment for the prevention of

thromboembolic stroke. However, our results and reports of patients with COL4A1 or COL4A2 mutations suffering from hemorrhagic stroke while taking anticoagulant medication suggest that the risks of antithrombotic therapy may be judged to outweigh its benefits.^{5,6,27,31} These decisions will need to be measured against the increased risk for ICH. Similarly, *Col4a1* mutations are not associated with hypertension^{27,44}; however, intense exercise in mice induced ICH and has been associated with hemorrhagic events in patients.^{28–30} These data are important for patients with COL4A1 and COL4A2 mutations who are considering the beneficial or detrimental consequences of physical exercise. Although cesarean delivery will not reduce or prevent embryonic ICH or pencephaly, our data demonstrate that cesarean delivery of genetically at-risk individuals may reduce perinatal ICH. Because of the exacerbating effects of intense exercise, cesarean delivery may also be warranted when the mother carries the mutation.

Conclusions

We used an allelic series, genetic modification, and a conditionally expressed *Col4a1* mutation to distinguish the relative impacts of intracellular accumulation from extracellular COL4A1 deficiency, to dissect cell type-specific contributions, and to define a window for potential therapeutic intervention. Our data suggest that intracellular collagen accumulation is responsible for ICH progression. Thus, promoting either heterotrimer degradation or secretion may be a viable approach to reduce ICH severity. Importantly, we show that 4PBA, a readily available small molecule with chaperone properties, reduced ICH severity in vivo. Together, these findings demonstrate the efficacy of controlling modifiable environmental risk factors and application of a mechanism-based therapy to prevent ICH caused by COL4A1 mutations.

Acknowledgments

We thank J. Rosand, R. Libby, R. Daneman, P. Yurchenco, and members of the Gould laboratory for critical reviews of the manuscript.

Sources of Funding

This study was funded by the American Heart Association, National Institutes of Health (NS083830), and That Man May See (Dr Gould). Support was also provided by an American Heart Association postdoctoral fellowship (Dr Jeanne) and by a core grant from the National Eye Institute (EY02162), a Research to Prevent Blindness unrestricted grant (Department of Ophthalmology, University of California, San Francisco), the Sandler Program in Basic Sciences (Dr Gould), and the Karl Kirchgessner Foundation (Dr Gould).

Disclosures

None.

References

- Go AS, Mozaffarian D, Roger VL, Benjamin EJ, Berry JD, Blaha MJ, Dai S, Ford ES, Fox CS, Franco S, Fullerton HJ, Gillespie C, Hailpern SM, Heit JA, Howard VJ, Huffman MD, Judd SE, Kissela BM, Kittner SJ, Lackland DT, Lichtman JH, Lisabeth LD, Mackey RH, Magid DJ, Marcus GM, Marelli A, Matchar DB, McGuire DK, Mohler ER 3rd, Moy CS, Mussolino ME, Neumar RW, Nichol G, Pandey DK, Paynter NP, Reeves MJ, Sorlie PD, Stein J, Towfighi A, Turan TN, Virani SS, Wong ND, Woo D, Turner MB; American Heart Association Statistics Committee and Stroke Statistics Subcommittee. Heart disease and stroke statistics—2014 update: a report from the American Heart Association. *Circulation*. 2014;129:e28–e292. doi: 10.1161/01.cir.0000441139.02102.80.

2. Qureshi AI, Tuhim S, Broderick JP, Batjer HH, Hondo H, Hanley DF. Spontaneous intracerebral hemorrhage. *N Engl J Med*. 2001;344:1450–1460. doi: 10.1056/NEJM200105103441907.
3. Kuo DS, Labelle-Dumais C, Gould DB. COL4A1 and COL4A2 mutations and disease: insights into pathogenic mechanisms and potential therapeutic targets. *Hum Mol Genet*. 2012;21:R97–R110. doi: 10.1093/hmg/ddc346.
4. Yoneda Y, Haginoya K, Arai H, Yamaoka S, Tsurusaki Y, Doi H, Miyake N, Yokochi K, Osaka H, Kato M, Matsumoto N, Saito H. De novo and inherited mutations in COL4A2, encoding the type IV collagen alpha2 chain cause porencephaly. *Am J Hum Genet*. 2012;90:86–90.
5. Jeanne M, Labelle-Dumais C, Jorgensen J, Kauffman WB, Mancini GM, Favor J, Valant V, Greenberg SM, Rosand J, Gould DB. COL4A2 mutations impair COL4A1 and COL4A2 secretion and cause hemorrhagic stroke. *Am J Hum Genet*. 2012;90:91–101. doi: 10.1016/j.ajhg.2011.11.022.
6. Weng YC, Sonni A, Labelle-Dumais C, de Leau M, Kauffman WB, Jeanne M, Biffi A, Greenberg SM, Rosand J, Gould DB. COL4A1 mutations in patients with sporadic late-onset intracerebral hemorrhage. *Ann Neurol*. 2012;71:470–477. doi: 10.1002/ana.22682.
7. Yurchenco PD, Amenta PS, Patton BL. Basement membrane assembly, stability and activities observed through a developmental lens. *Matrix Biol*. 2004;22:521–538. doi: 10.1016/j.matbio.2003.10.006.
8. Yurchenco PD, Ruben GC. Basement membrane structure in situ: evidence for lateral associations in the type IV collagen network. *J Cell Biol*. 1987;105(pt 1):2559–2568.
9. Khoshnoodi J, Sigmondsson K, Cartiailler JP, Bondar O, Sundaramoorthy M, Hudson BG. Mechanism of chain selection in the assembly of collagen IV: a prominent role for the alpha2 chain. *J Biol Chem*. 2006;281:6058–6069. doi: 10.1074/jbc.M50655200.
10. Dixit SN, Stuart JM, Seyer JM, Risteli J, Timpl R, Kang AH. Type IV collagens' isolation and characterization of 7S collagen from human kidney, liver and lung. *Coll Relat Res*. 1981;1:549–556.
11. Trüeb B, Gröbli B, Spiess M, Odermatt BF, Winterhalter KH. Basement membrane (type IV) collagen is a heteropolymer. *J Biol Chem*. 1982;257:5239–5245.
12. Ries A, Engel J, Lustig A, Kühn K. The function of the NC1 domains in type IV collagen. *J Biol Chem*. 1995;270:23790–23794.
13. Boutaud A, Borza DB, Bondar O, Gunwar S, Netzer KO, Singh N, Ninomiya Y, Sado Y, Noelken ME, Hudson BG. Type IV collagen of the glomerular basement membrane: evidence that the chain specificity of network assembly is encoded by the noncollagenous NC1 domains. *J Biol Chem*. 2000;275:30716–30724. doi: 10.1074/jbc.M004569200.
14. Kuivaniemi H, Tromp G, Prockop DJ. Mutations in collagen genes: causes of rare and some common diseases in humans. *FASEB J*. 1991;5:2052–2060.
15. Prockop DJ, Kivirikko KI. Heritable diseases of collagen. *N Engl J Med*. 1984;311:376–386. doi: 10.1056/NEJM198408093110606.
16. Engel J, Prockop DJ. The zipper-like folding of collagen triple helices and the effects of mutations that disrupt the zipper. *Annu Rev Biophys Biophys Chem*. 1991;20:137–152. doi: 10.1146/annurev.bb.20.060191.001033.
17. Gould DB, Phalan FC, Breedveld GJ, van Mil SE, Smith RS, Schimenti JC, Aguglia U, van der Knaap MS, Heutink P, John SW. Mutations in Col4a1 cause perinatal cerebral hemorrhage and porencephaly. *Science*. 2005;308:1167–1171. doi: 10.1126/science.1109418.
18. Kuo DS, Labelle-Dumais C, Mao M, Jeanne M, Kauffman WB, Allen J, Favor J, Gould DB. Allelic heterogeneity contributes to variability in ocular dysgenesis, myopathy and brain malformations caused by Col4a1 and Col4a2 mutations. *Hum Mol Genet*. 2014;23:1709–1722. doi: 10.1093/hmg/ddt560.
19. Marini JC, Forlino A, Cabral WA, Barnes AM, San Antonio JD, Milgrom S, Hyland JC, Körkkö J, Prockop DJ, De Paeppe A, Coucke P, Symoens S, Glorieux FH, Roughley PJ, Lund AM, Kuurila-Svahn K, Hartikka H, Cohn DH, Krakow D, Mottes M, Schwarze U, Chen D, Yang K, Kuslich C, Troendle J, Dalglish R, Byers PH. Consortium for osteogenesis imperfecta mutations in the helical domain of type I collagen: regions rich in lethal mutations align with collagen binding sites for integrins and proteoglycans. *Hum Mutat*. 2007;28:209–221. doi: 10.1002/humu.20429.
20. Favor J, Gloeckner CJ, Janik D, Klempt M, Neuhauser-Klaus A, Pretsich W, Schmahl W, Quintanilla-Fend L. Type IV procollagen missense mutations associated with defects of the eye, vascular stability, the brain, kidney function and embryonic or postnatal viability in the mouse, *Mus musculus*: an extension of the Col4a1 allelic series and the identification of the first two Col4a2 mutant alleles. *Genetics*. 2007;175:725–736.
21. Badea TC, Wang Y, Nathans J. A noninvasive genetic/pharmacologic strategy for visualizing cell morphology and clonal relationships in the mouse. *J Neurosci*. 2003;23:2314–2322.
22. Kisanuki YY, Hammer RE, Miyazaki J, Williams SC, Richardson JA, Yanagisawa M. Tie2-Cre transgenic mice: a new model for endothelial cell-lineage analysis in vivo. *Dev Biol*. 2001;230:230–242. doi: 10.1006/dbio.2000.0106.
23. Foo SS, Turner CJ, Adams S, Compagni A, Aubyn D, Kogata N, Lindblom P, Shani M, Zicha D, Adams RH. Ephrin-B2 controls cell motility and adhesion during blood-vessel-wall assembly. *Cell*. 2006;124:161–173. doi: 10.1016/j.cell.2005.10.034.
24. Zhuo L, Theis M, Alvarez-Maya I, Brenner M, Willecke K, Messing A. hGFAP-cre transgenic mice for manipulation of glial and neuronal function in vivo. *Genesis*. 2001;31:85–94.
25. Madisen L, Zwingman TA, Sunkin SM, Oh SW, Zariwala HA, Gu H, Ng LL, Palmiter RD, Hawrylycz MJ, Jones AR, Lein ES, Zeng H. A robust and high-throughput Cre reporting and characterization system for the whole mouse brain. *Nat Neurosci*. 2010;13:133–140. doi: 10.1038/nn.2467.
26. Sado Y, Kagawa M, Kishiro Y, Sugihara K, Naito I, Seyer JM, Sugimoto M, Oohashi T, Ninomiya Y. Establishment by the rat lymph node method of epitope-defined monoclonal antibodies recognizing the six different alpha chains of human type IV collagen. *Histochem Cell Biol*. 1995;104:267–275.
27. Gould DB, Phalan FC, van Mil SE, Sundberg JP, Vahedi K, Massin P, Bousser MG, Heutink P, Miner JH, Tournier-Lasserre E, John SW. Role of COL4A1 in small-vessel disease and hemorrhagic stroke. *N Engl J Med*. 2006;354:1489–1496. doi: 10.1056/NEJMoa053727.
28. Vahedi K, Kubis N, Boukobza M, Arnoult M, Massin P, Tournier-Lasserre E, Bousser MG. COL4A1 mutation in a patient with sporadic, recurrent intracerebral hemorrhage. *Stroke*. 2007;38:1461–1464. doi: 10.1161/STROKEAHA.106.475194.
29. Gunda B, Mine M, Kovács T, Hornyák C, Bereczki D, Várallyay G, Rudas G, Audrezet MP, Tournier-Lasserre E. COL4A2 mutation causing adult onset recurrent intracerebral hemorrhage and leukoencephalopathy. *J Neurol*. 2014;261:500–503. doi: 10.1007/s00415-013-7224-4.
30. Corro A, Tournier-Lasserre E, Mine M, Menjot de Champfleury N, Carla Dalliere C, Ayrganac X, Labauge P, Arquisin C. COL4A1 mutation revealed by an isolated brain hemorrhage. *Cerebrovasc Dis*. 2013;35:593–594. doi: 10.1159/000351520.
31. Alamowitch S, Plaisier E, Favrole P, Prost C, Chen Z, Van Agtmael T, Marro B, Ronco P. Cerebrovascular disease related to COL4A1 mutations in HANAC syndrome. *Neurology*. 2009;73:1873–1882. doi: 10.1212/WNL.0b013e3181c3fd12.
32. Gould DB, Marchant JK, Savinova OV, Smith RS, John SW. Col4a1 mutation causes endoplasmic reticulum stress and genetically modifiable ocular dysgenesis. *Hum Mol Genet*. 2007;16:798–807. doi: 10.1093/hmg/ddm024.
33. Labelle-Dumais C, Dilworth DJ, Harrington EP, de Leau M, Lyons D, Kabaeva S, Manzini MC, Dobyns WB, Walsh CA, Michele DE, Gould DB. COL4A1 mutations cause ocular dysgenesis, neuronal localization defects, and myopathy in mice and Walker-Warburg syndrome in humans. *PLoS Genet*. 2011;7:e1002062. doi: 10.1371/journal.pgen.1002062.
34. Starman BJ, Eyre D, Charbonneau H, Harrylock M, Weis MA, Weiss L, Graham JM Jr, Byers PH. Osteogenesis imperfecta: the position of substitution for glycine by cysteine in the triple helical domain of the pro alpha 1(I) chains of type I collagen determines the clinical phenotype. *J Clin Invest*. 1989;84:1206–1214. doi: 10.1172/JCI114286.
35. Byers PH, Wallis GA, Willing MC. Osteogenesis imperfecta: translation of mutation to phenotype. *J Med Genet*. 1991;28:433–442.
36. Willing MC, Deschenes SP, Scott DA, Byers PH, Slayton RL, Pitts SH, Arikat H, Roberts EJ. Osteogenesis imperfecta type I: molecular heterogeneity for COL1A1 null alleles of type I collagen. *Am J Hum Genet*. 1994;55:638–647.
37. Iannitti T, Palmieri B. Clinical and experimental applications of sodium phenylbutyrate. *Drugs R D*. 2011;11:227–249. doi: 10.2165/11591280-000000000-00000.
38. Murray LS, Lu Y, Taggart A, Van Regemorter N, Vilain C, Abramowicz M, Kadler KE, Van Agtmael T. Chemical chaperone treatment reduces intracellular accumulation of mutant collagen IV and ameliorates the cellular phenotype of a COL4A2 mutation that causes haemorrhagic stroke. *Hum Mol Genet*. 2014;23:283–292. doi: 10.1093/hmg/ddt418.
39. Paralkar VM, Vukicevic S, Reddi AH. Transforming growth factor beta type 1 binds to collagen IV of basement membrane matrix: implications for development. *Dev Biol*. 1991;143:303–308.
40. Wang X, Harris RE, Bayston LJ, Ashe HL. Type IV collagens regulate BMP signalling in *Drosophila*. *Nature*. 2008;455:72–77. doi: 10.1038/nature07214.

41. Zhang X, Meng H, Wang MM. Collagen represses canonical Notch signaling and binds to Notch ectodomain. *Int J Biochem Cell Biol.* 2013;45:1274–1280. doi: 10.1016/j.biocel.2013.03.020.
42. Venstrom K, Reichardt L. Beta 8 integrins mediate interactions of chick sensory neurons with laminin-1, collagen IV, and fibronectin. *Mol Biol Cell.* 1995;6:419–431.
43. Colorado PC, Torre A, Kamphaus G, Maeshima Y, Hopfer H, Takahashi K, Volk R, Zamborsky ED, Herman S, Sarkar PK, Ericksen MB, Dhanabal M, Simons M, Post M, Kufe DW, Weichselbaum RR, Sukhatme VP, Kalluri R. Anti-angiogenic cues from vascular basement membrane collagen. *Cancer Res.* 2000;60:2520–2526.
44. Van Agtmael T, Bailey MA, Schlötzer-Schrehardt U, Craigie E, Jackson IJ, Brownstein DG, Megson IL, Mullins JJ. Col4a1 mutation in mice causes defects in vascular function and low blood pressure associated with reduced red blood cell volume. *Hum Mol Genet.* 2010;19:1119–1128. doi: 10.1093/hmg/ddp584.

CLINICAL PERSPECTIVE

Despite intracerebral hemorrhage (ICH) being the most fatal form of stroke, there is a lack of effective treatment options, and only a few genetic causes have been identified. Mutations in the collagen type IV alpha1 (*COL4A1*) and alpha2 (*COL4A2*) genes cause highly penetrant cerebrovascular disease, including porencephaly, perinatal ICHs, small-vessel disease, and recurrent spontaneous ICHs in adults. Using *Col4a1* mutant mice modeling human disease, we showed that the pathogenesis occurs in different phases, with age-related ICHs and macroangiopathy being consequences of abnormal vascular development. Our data suggest that toxic intracellular collagen accumulation in the abnormal vasculature is a key pathogenic event that leads to ICH progression. Using sodium 4-phenylbutyrate, a US Food and Drug Administration–approved drug with chemical chaperone properties, we showed that targeting this event in our mouse model, even after birth, successfully decreases ICH severity in vivo. We also discovered important allelic effects, with mutation class, domain, and position all influencing ICH severity. We recommend considering them when functionally testing putative mutations identified in ICH patients because mutations near the amino terminus may cause only mild intracellular collagen accumulation, resulting in false negatives. Showing that position-matched mutations in *Col4a1* and *Col4a2* caused similar ICH severity, our results also stress the importance of analyzing both genes when genetically screening patients. Finally, we found that vaginal delivery, intense exercise, and anticoagulant use exacerbate ICH severity. We propose that controlling these modifiable environmental risk factors and targeting intracellular collagen accumulation are viable approaches for stroke prevention in patients with *COL4A1* and *COL4A2* mutations.

Molecular and Genetic Analyses of Collagen Type IV Mutant Mouse Models of Spontaneous Intracerebral Hemorrhage Identify Mechanisms for Stroke Prevention

Marion Jeanne, Jeff Jorgensen and Douglas B. Gould

Circulation. 2015;131:1555-1565; originally published online March 9, 2015;

doi: 10.1161/CIRCULATIONAHA.114.013395

Circulation is published by the American Heart Association, 7272 Greenville Avenue, Dallas, TX 75231

Copyright © 2015 American Heart Association, Inc. All rights reserved.

Print ISSN: 0009-7322. Online ISSN: 1524-4539

The online version of this article, along with updated information and services, is located on the World Wide Web at:

<http://circ.ahajournals.org/content/131/18/1555>

Data Supplement (unedited) at:

<http://circ.ahajournals.org/content/suppl/2015/03/09/CIRCULATIONAHA.114.013395.DC1>

Permissions: Requests for permissions to reproduce figures, tables, or portions of articles originally published in *Circulation* can be obtained via RightsLink, a service of the Copyright Clearance Center, not the Editorial Office. Once the online version of the published article for which permission is being requested is located, click Request Permissions in the middle column of the Web page under Services. Further information about this process is available in the [Permissions and Rights Question and Answer](#) document.

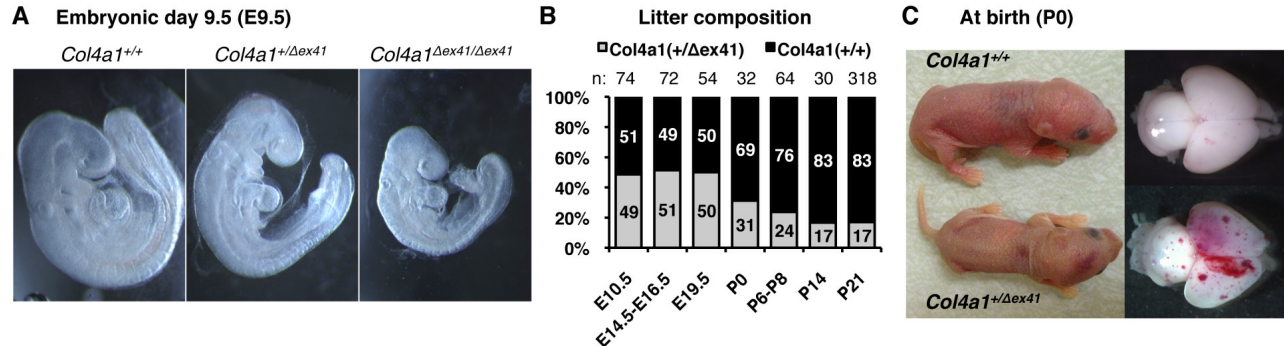
Reprints: Information about reprints can be found online at:
<http://www.lww.com/reprints>

Subscriptions: Information about subscribing to *Circulation* is online at:
<http://circ.ahajournals.org/subscriptions/>

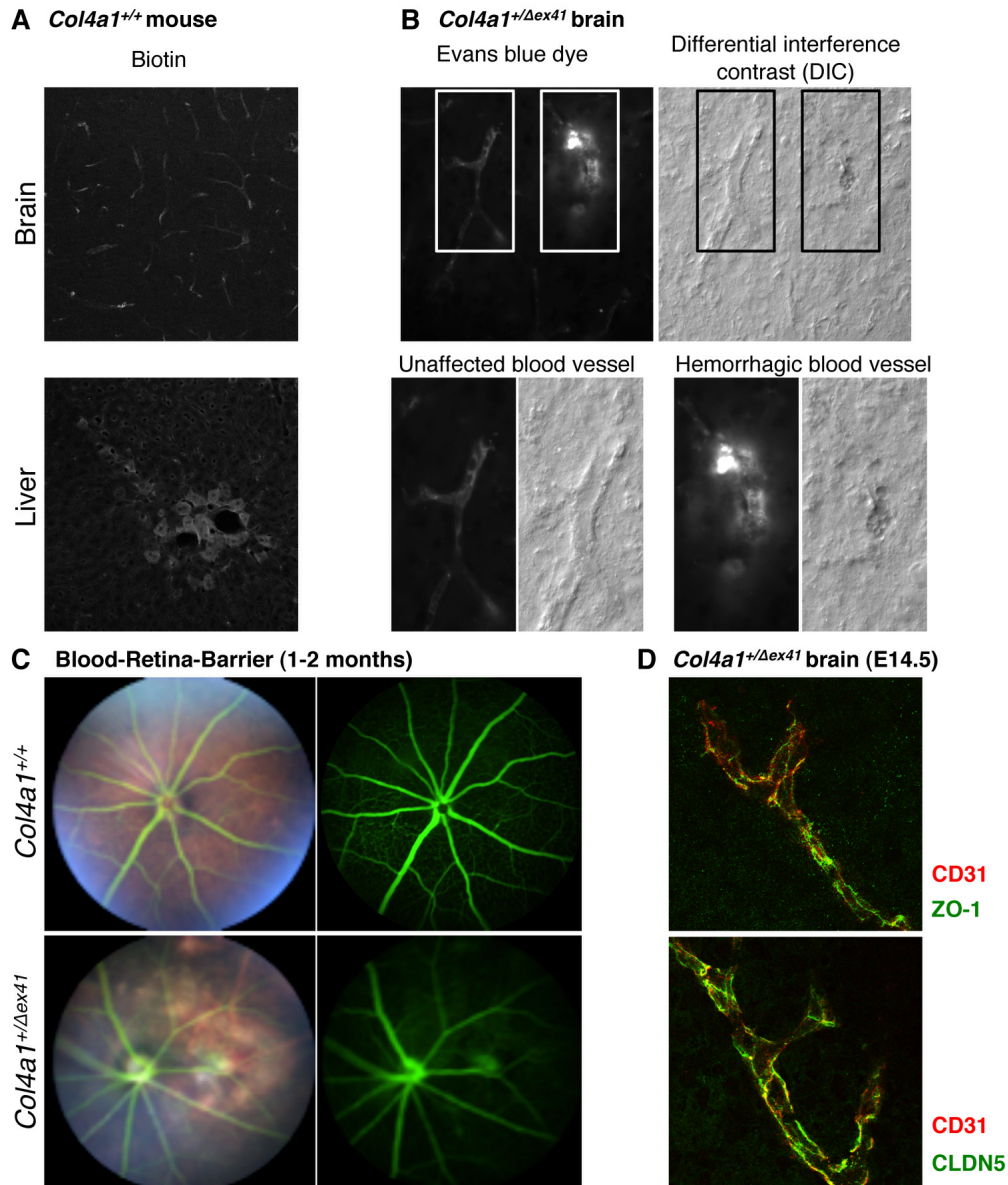
SUPPLEMENTAL MATERIAL (Supplemental Figures 1 to 8)

“Molecular and Genetic Analysis of Collagen Type IV Mutant Mouse Models of Spontaneous Intracerebral Hemorrhage Identify Mechanisms for Stroke Prevention”

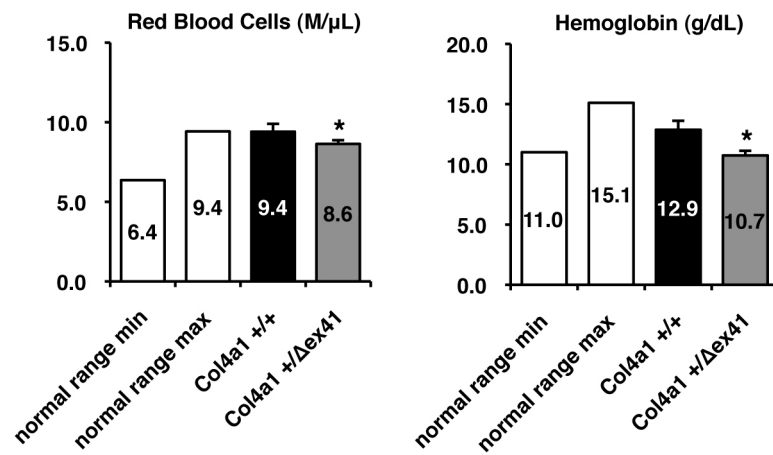
Marion Jeanne, Jeff Jorgensen, Douglas B. Gould



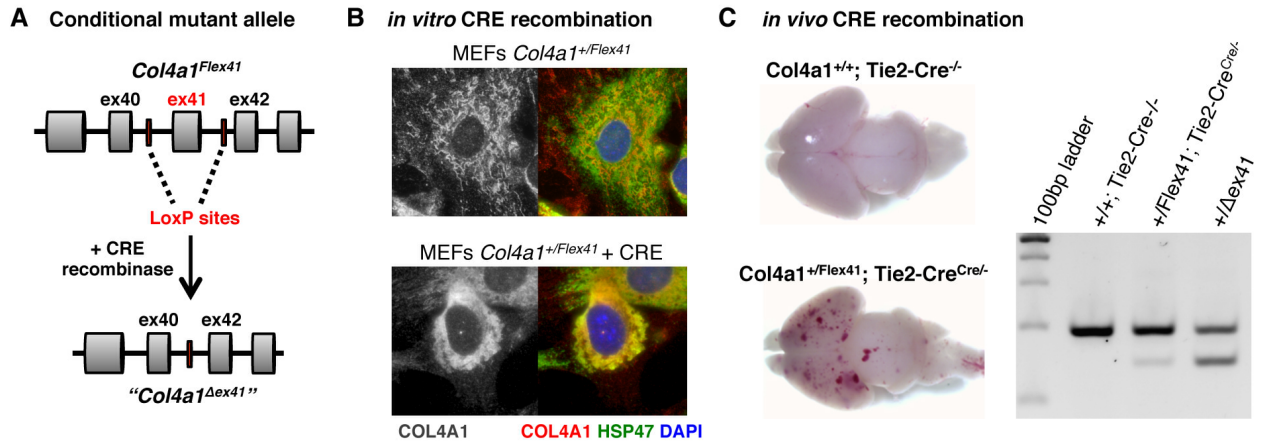
Supplemental Figure 1: *Col4a1* ^{Δ ex41} causes embryonic growth retardation, reduced viability and multifocal hemorrhages (A) Growth retardation is observed in *Col4a1*^{+/ Δ ex41} mutants as early as embryonic day (E) 9.5 and is more pronounced in homozygous *Col4a1* ^{Δ ex41/ Δ ex41} mutants, which do not survive after mid-gestation. (B) In backcross matings, mutant embryos are represented at expected ratios of 1:1 until birth when *Col4a1*^{+/ Δ ex41} mice have reduced viability (n: number of animals for each time point). (C) At birth (postnatal day 0: P0), *Col4a1*^{+/ Δ ex41} pups have multi-focal subcutaneous hematomas and intraparenchymal hemorrhages.



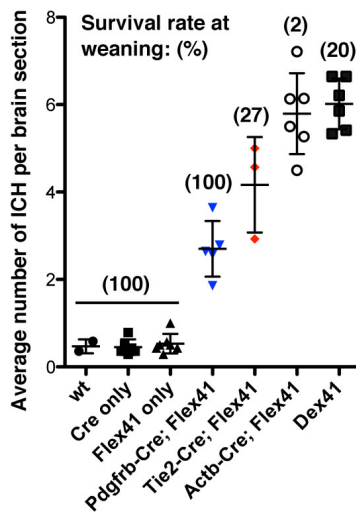
Supplemental Figure 2: Blood-brain-barrier and blood-retina-barrier are not compromised in *Col4a1*^{+/ Δ ex41} animals (A) As a positive control for the experiment presented in Figure 1 (D), we show that biotin diffuses from the blood vessel into the liver (bottom) whereas it stays inside the cerebral vasculature (top) because of the presence of the blood-brain-barrier in a *Col4a1*^{+/+} mouse (B) In *Col4a1*^{+/ Δ ex41} mice, intracardiac perfusion of biotin revealed that the blood-brain-barrier is intact (unaffected blood vessel) until the vasculature ruptures, leading to hemorrhage and leakage of biotin in the surrounding parenchyma (hemorrhagic blood vessel) (C) Intra-peritoneal injection of sodium fluorescein reveals no general leakage of the *Col4a1*^{+/ Δ ex41} blood-retina-barrier on ocular fundus examination. (D) Blood-brain-barrier proteins such as zona occludens protein 1 (ZO-1) and Claudin 5 (CLDN5) (labeled in green) are expressed in *Col4a1*^{+/ Δ ex41} cerebral blood vessels (labeled with CD31, red) as early as E14.5.



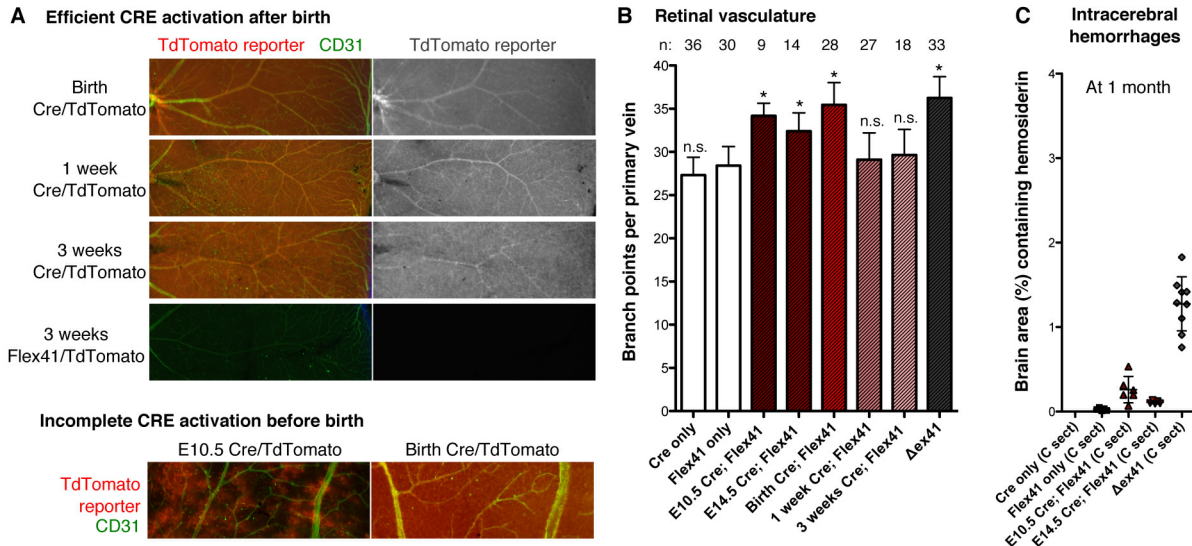
Supplemental Figure 3: *Col4a1*^{+/-Δex41} mice have anemia. Blood analysis at 4 months shows decreased number of red blood cells and abnormally low hemoglobin level in *Col4a1*^{+/-Δex41} (n=5) compared to *Col4a1*^{+/+} mice (n=9). Data are reported as mean + standard deviation. *: p<0.05 compared to *Col4a1*^{+/+} mice by Student's t-test.



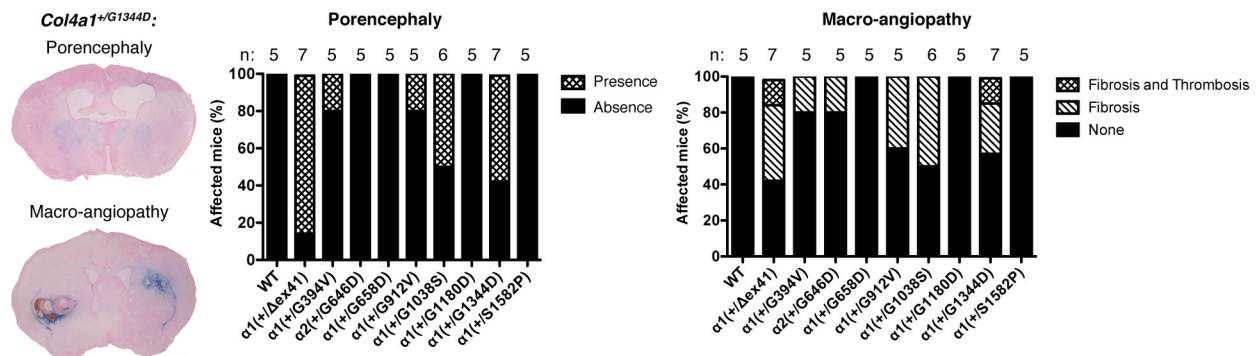
D E16.5 Intracerebral hemorrhages



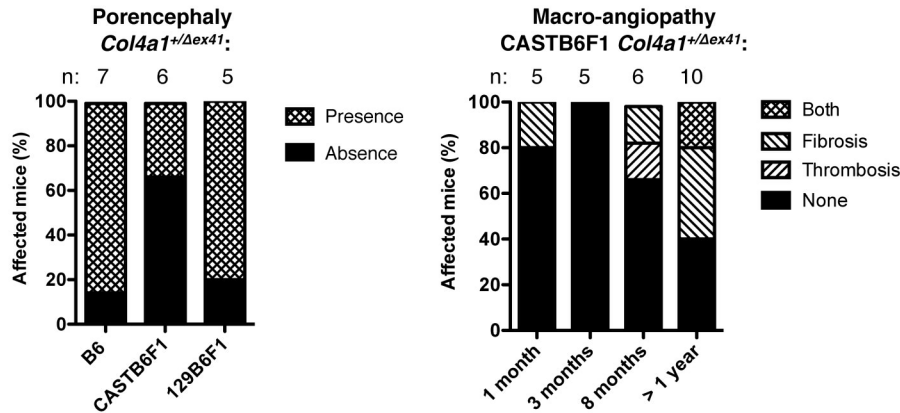
Supplemental Figure 4: The *Col4a1*^{Flex41} conditional mutant allele in presence of active CRE recombinae mimics the *Col4a1*^{Δex41} mutation (A) The *Col4a1*^{Flex41} conditional mutant allele has exon 41 flanked by *LoxP* sites. In the presence of active CRE recombinae, exon 41 is removed, mimicking pathogenic effects of the *Col4a1*^{Δex41} mutation such as (B) intracellular accumulation of collagen in the endoplasmic reticulum (ER) (MEFs: primary mouse embryonic fibroblasts, HSP47: ER marker). (C) Compared to littermate controls that did not have hemorrhage, double heterozygous *Col4a1*^{+/*Flex41*}; *Tie2-Cre*^{CRE/-} (endothelial-specific expression of CRE) P0 pups showed perinatal multi-focal intracerebral hemorrhage (ICH). cDNA from whole brain amplified with primers in *Col4a1* exons 40 and 42 detected expression of transcripts missing exon 41 (51 nucleotides) in *Col4a1*^{+/*Flex41*} mice when CRE is present (lower band). (D) Average number of ICHs per brain section in E16.5 embryos. *Col4a1*^{+/*Flex41*}; *Actb-Cre*^{CRE/-} embryos, expressing CRE recombinae ubiquitously have as many ICH as *Col4a1*^{+/*Δex41*} embryos. The survival rate at weaning age is indicated (%). Data are reported as mean ± standard deviation.



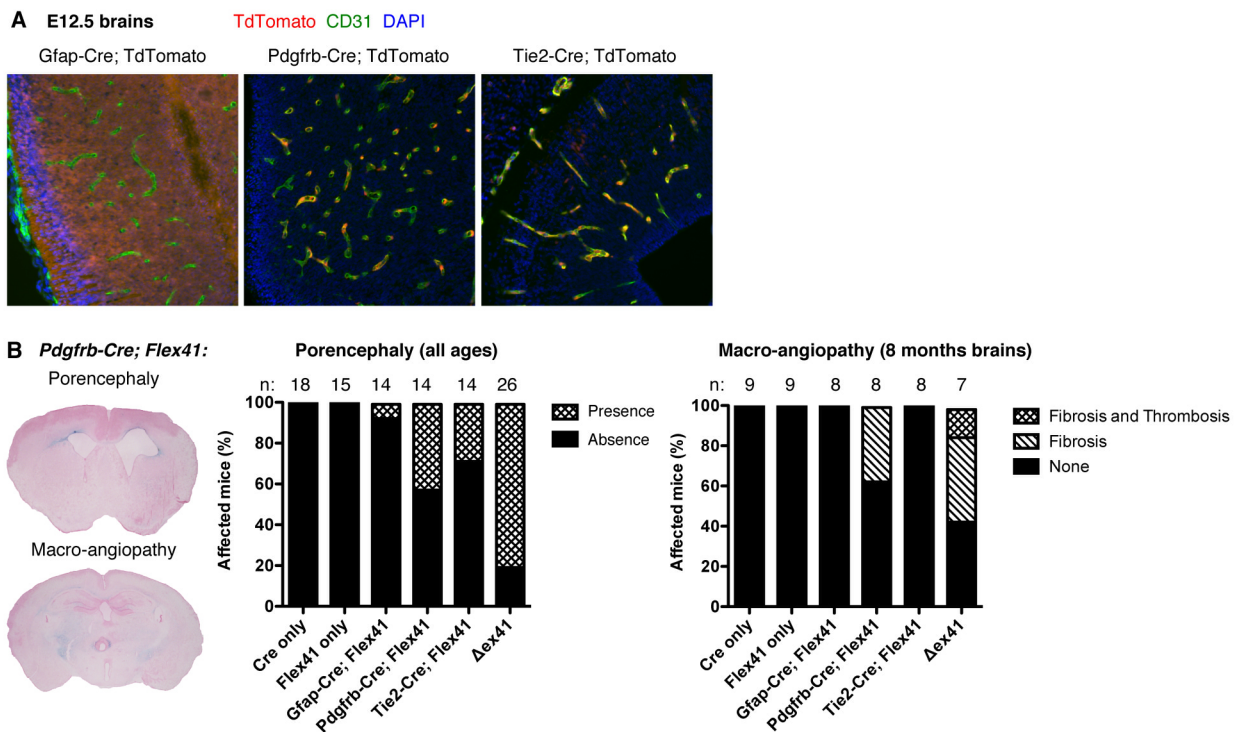
Supplemental Figure 5: Tamoxifen induces ubiquitous CRE activation when injected after birth, but only partial CRE activation when injected during gestation (A) We evaluated the efficiency of CRE activation by tamoxifen using the TdTomato reporter mouse strain. Postnatal tamoxifen injection achieved ostensibly complete recombination whereas prenatal tamoxifen injection did not (TdTomato in red, CD31 in green) **(B)** Quantification of retinal vein branch points showed excess branching when tamoxifen was delivered before or at birth but not after one week (when retinal vascular development is completed) confirming that tamoxifen delivery and mutant *Col4a1* induction was successful ($9 \leq n \leq 36$). n.s.: $p > 0.05$, *: $p < 0.05$ compared to Flex41 only (*Col4a1*^{+/*Flex41*}; *R26CreER*^{-/-}) mice by Student's *t*-test. **(C)** Intracerebral hemorrhage (ICH) quantification of brains from 1-month old mice showed that mutant *Col4a1* induction at E10.5 or E14.5 caused ICH and that earlier induction led to more ICH. Tamoxifen administration compromised natural birth so all litters were surgically delivered (C sect). The observation that E10.5 induction did not phenocopy *Col4a1*^{+/*Δex41*} mice likely reflects the reduced recombination efficiency shown in A. Data are reported as mean + (B) or ± (C) standard deviation.



Supplemental Figure 6: Porencephaly and macro-angiopathy in an allelic series of *Col4a1* and *Col4a2* mutations. We analyzed 27 regularly spaced coronal cryo-sections per brain ($n=5-7$ mice per genotype) to determine the frequencies of porencephaly and macro-angiopathy in mice from the allelic series.



Supplemental Figure 7: CASTB6F1 genetic context prevents or delays cerebrovascular disease caused by *Col4a1^{Δex41}* mutation. The penetrance of porencephaly in *Col4a1^{+/Δex41}* mice was reduced by CASTB6F1 but not 129B6F1 genetic context. CASTB6F1 also prevents or delays macro-angiopathy in *Col4a1^{+/Δex41}* mice. C57BL/6J (B6), CAST/EiJ (CAST), 129S6/SvEvTac (129) (n: number of animals in each cohort).



Supplemental Figure 8: Cell type specific expression of mutant COL4A1 (A) Cell type specific CRE mouse strains were crossed with a TdTomato reporter strain to show the specificity of the CRE expression: in astrocytes, in pericytes and in vascular endothelial cells (VECs) for *Gfap-Cre*, *Pdgfrb-Cre* and *Tie2-Cre* respectively (CD31 labeled the VECs in green, TdTomato is red in cells expressing the CRE, brain sections of embryonic day 12.5 embryos) **(B)** Porencephaly and macro-angiopathy penetrance were quantified using serial coronal brain sections (n: number of animals in each cohort).